HHS Public Access

Author manuscript

Mol Microbiol. Author manuscript; available in PMC 2018 November 01.

Published in final edited form as:

Mol Microbiol. 2017 November ; 106(3): 367–380. doi:10.1111/mmi.13770.

Viscous drag on the flagellum activates *Bacillus subtilis* entry into the K-state

Christine Diethmaier[1], **Ravi Chawla**[2], **Alexandra Canzoneri**[3], **Daniel B. Kearns**[3], **Pushkar P. Lele**[2], and **David Dubnau**[1]

[1]Public Health Research Institute Center, New Jersey Medical School, Rutgers University, Newark, NJ, USA

[2]Artie McFerrin Department of Chemical Engineering, Texas A&M University, College Station Texas, USA

[3]Department of Biology, Indiana University, Bloomington, Indiana, USA

Abstract

Bacillus subtilis flagella are not only required for locomotion but also act as sensors that monitor environmental changes. Although how the signal transmission takes place is poorly understood, it has been shown that flagella play an important role in surface sensing by transmitting a mechanical signal to control the DegS-DegU two-component system. Here we report a role for flagella in the regulation of the K-state, which enables transformability and antibiotic tolerance (persistence). Mutations impairing flagellar synthesis are inferred to increase DegU-P, which inhibits the expression of ComK, the master regulator for the K-state, and reduces transformability. Tellingly, both deletion of the flagellin gene and straight filament (*hag*^{A233V}) mutations increased DegU phosphorylation despite the fact that both mutants had wild type numbers of basal bodies and the flagellar motors were functional. We propose that higher viscous loads on flagellar motors result in lower DegU-P levels through an unknown signaling mechanism. This flagellar-load based mechanism ensures that cells in the motile subpopulation have a 10-fold enhanced likelihood of entering the K-state and taking up DNA from the environment. Further, our results suggest that the developmental states of motility and competence are related and most commonly occur in the same epigenetic cell type.

Graphical Abstract

Viscous load on rotating flagella signals to lower the amount of DegU-P. This in turn increases the probability that *Bacillus subtilis* will enter the K-state.

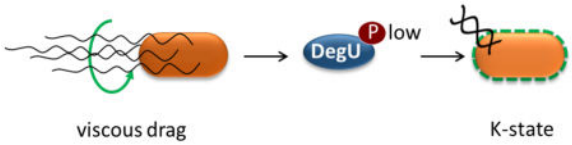

*For correspondence. dubnauda@njms.rutgers.edu.

Keywords

flagella; K-state; hag; DegU-P; viscous load

Introduction

The most evident role for the rotary bacterial flagellum is in cell motility and chemotaxis (Berg & Brown, 1972, Adler, 1975, Purcell, 1977, Armitage, 1992). Remarkably, these molecular machines can also serve a sensory function, by detecting surface interactions to initiate the expression of biofilm genes (Belas, 2014, Ellison & Brun, 2015). The earliest evidence for a flagellar mechanosensory role is in the control of swarming in *Vibrio parahaemolyticus* (Belas *et al.*, 1986, McCarter *et al.*, 1988). In *Vibrio cholerae*, proper motor rotation is critical for permanent cell attachment, perhaps because flagellar interaction with a surface results in hyperpolarization of the membrane, an event that is correlated with attachment (Van Dellen *et al.*, 2008). In *Pseudomonas aeruginosa*, the reversal frequency of flagella rotation plays a role in biofilm formation (Caiazza & O'Toole, 2004, Caiazza *et al.*, 2007), while in *Caulobacter crescentus*, inhibition of flagella rotation initiates adhesion to a surface by stimulating holdfast synthesis (Li *et al.*, 2012). Recent work in *Escherichia coli* suggests that within the motor, it is the stator (the torque-generating protein complex) that functions as a mechanosensor (Lele *et al.*, 2013, Tipping *et al.*, 2013, Che *et al.*, 2014). Upon sensing an increase in the viscous load, the stator-complex recruits additional stator-units (Lele *et al.*, 2013, Tipping *et al.*, 2013). Although the mechanisms are unknown at present, stator-remodeling might be one way in which some bacterial species adapt to a surface-associated lifestyle.

In the Gram-positive model organism *Bacillus subtilis*, flagellar defects appear to cause the accumulation of the phosphorylated transcription factor DegU-P, resulting in the transcriptional up-regulation of poly-γ-glutamate synthesis (Cairns *et al.*, 2013, Chan *et al.*, 2014). It has been proposed that in the wild-type, interaction with a surface perturbs flagellar rotation and up-regulates genes needed for biofilm formation, including those dependent on DegU-P (Cairns *et al.*, 2013). During the process of biofilm formation, the protein EpsE is synthesized, acting both as an essential enzyme for the production of the extracellular matrix and as a clutch, disengaging the flagellum from its motor and contributing to the transition from a motile to a sessile state (Blair *et al.*, 2008, Guttenplan *et al.*, 2010). Thus, flagellar rotation is intimately related to the formation of the *B. subtilis* biofilm at multiple levels.

B. subtilis contains typical ion-driven flagella, consisting of three architectural domains: the basal body, the hook and the filament (Berg, 2003, Chevance & Hughes, 2008, Minamino *et al.*, 2008, Guttenplan *et al.*, 2013, Mukherjee & Kearns, 2014). The filament is helical and is composed of repeating units of the protein flagellin, encoded by *hag*. The hook, a distinct structure, is located at the base of the filament and is also attached to the basal body, located in the cell envelope. The motor included in the basal body contains two functional entities; the rotor and the proton-conducting stator complex built by MotA and MotB (Block & Berg, 1984, Kojima & Blair, 2004). Protonation of the Asp24 residue in the *B. subtilis* MotB is thought to cause conformational changes in the cytoplasmic region of MotA, generating a

torque at the rotor interface (the FliG ring) (Kojima & Blair, 2001, Cairns *et al.*, 2013, Chan *et al.*, 2014). Torque is then imparted to the filament through the rod, causing the flagellum to rotate.

While previous work in *B. subtilis* highlighted the role of flagella as mechanosensors for surface contact (Cairns *et al.*, 2013) and for the induction of poly-γ-glutamate synthesis (Chan *et al.*, 2014), we report a previously unrecognized effect of flagellar signaling in the regulation of the K-state. The K-state refers to a physiological condition in which ComK is expressed, along with about 100 genes dependent for their transcription on ComK (van Sinderen *et al.*, 1995, Berka *et al.*, 2002, Hamoen *et al.*, 2002, Ogura *et al.*, 2002).. Among the proteins encoded by these genes are those that enable the uptake and processing of transforming DNA; K-state cells are thus genetically competent for transformation. In addition, K-state cells are arrested for growth and division and are tolerant of a number of antibiotics (Hahn *et al.*, 2015). Importantly, the K-state is bistably expressed, turning on in a subpopulation of cells. We show that mutations impairing flagella synthesis are less transformable due to the decreased basal expression of *comK* The lowering of the basal transcription rate, caused by the accumulation of DegU-P, results in a decreased frequency of transitions to the bistably expressed K-state (Mirouze *et al.*, 2012). In addition to confirming that flagella function suppresses DegU-P, we show that the generation of this signal is dependent on the viscous drag experienced by the flagellar motor. We propose that increased viscous loads on the motor depress DegU phosphorylation, perhaps as a consequence of motor remodeling. This mechanism ensures that K-state development takes place predominantly in the motile sub-population of *B. subtilis* cells.

Results

comK transcription is low in the absence of flagella

We observed that a deletion of the entire *fla/che* operon reduces the transcription rate from the P_{comK} promoter about 10-fold, shown using a promoter fusion to firefly luciferase as a reporter (Fig. 1A). The *fla/che* operon encodes many genes required for the synthesis of flagella and in its absence, motors, hooks and filaments are not produced (Zuberi *et al.*, 1990, Marquez-Magana & Chamberlin, 1994, Mukherjee & Kearns, 2014). Additionally, we replaced the native promoter of the *fla/che* operon by an isopropyl-β-D-thiogalactoside (IPTG)-inducible $P_{hyperspank}$ promoter and measured *comK* expression in the absence or presence of different IPTG concentrations (Fig. 1B). *comK* expression was reduced in the absence of induction and increased in the presence of IPTG in a dose-dependent manner until it reached a maximum at 0.1 mM IPTG. In these experiments, carried out in the undomesticated ancestral strain 3610, *comK* expression peaked at the time of entry into the stationary phase (T_0) at intermediate concentrations of IPTG, showing that the normal growth stage regulation of *comK* is unperturbed by the *fla/che* deletion.

The inactivation of *hag* or of *motB* also lowers *comK* expression

To determine whether the absence of individual flagellar components mimics that of the entire *fla/che* operon, we tested strains that were deleted for genes required for the most downstream flagellar components, *hag* or *motB*, which encode the flagellar filament and a

stator protein that powers filament rotation. Both of these strains exhibited reductions in *comK* expression indistinguishable from that of the *fla/che* deletant (Fig. 2A). Consistent with this, the *hag* mutant (Table 1) was less transformable than the wild-type strain. Because the K-state is normally expressed in a subpopulation (Maamar & Dubnau, 2005, Suel *et al.*, 2006, Maamar *et al.*, 2007), we used a fusion of the *comG* promoter to yellow fluorescent protein (YFP) to determine whether fewer cells expressed this ComK-dependent promoter in the *hag* strain. Microscopic enumeration of $P_{comG\text{-}yfp}$ expressing cells in the mutant and wild-type populations demonstrated about 10-fold fewer K-state cells in the *hag* strain than in the wild-type (Fig. 2C). In contrast, a non-polar deletion of *cheA*, a chemotaxis gene embedded in the *fla/che* operon, had no effect on K-state expression (not shown), suggesting that the chemotactic response is not needed for regulation. We conclude that the probability of transitions to the K-state is augmented by a signal that requires fully assembled and rotating flagella.

Deletion of *hag*, like that of *motB*, is inferred to raise the level of DegU-P

It has been shown in *B. subtilis* that flagella are not only important for motility, but act as mechanosensors to regulate exoprotease and poly-γ-glutamate synthesis on the level of gene expression by controlling the level of the phosphorylated response regulator protein, DegU-P (Cairns *et al.*, 2013, Chan *et al.*, 2014). It was proposed that the inhibition of flagellar rotation or of proton flux through MotB somehow signaled an increase in DegU-P, resulting in increased synthesis of poly-γ-glutamate in *motB* mutants (Cairns *et al.*, 2013). Based on these findings, we suspected that an increase in DegU-P might be responsible for the phenotypes reported above, although it would seem that the elimination of *hag* may not lead to the cessation of hook rotation or to an interruption of proton flow, because the hook and stator assemblies would remain intact. To assess the level of DegU-P in the *hag* strain, we used DegU-P dependent promoter fusions as well as mutations in *degU* and its cognate histidine kinase, *degS*. Transcription of the alkaline protease subtilisin, encoded by *aprE*, is activated by high DegU-P (Dahl *et al.*, 1992, Verhamme *et al.*, 2007, Murray *et al.*, 2009). To measure *aprE* transcription in the *hag* knockout, we used a promoter fusion of *aprE* to the luciferase gene and followed the expression of the P_{aprE} during growth in *hag* and wild-type cells. As shown in Fig. 3, the inactivation of *hag* increased the expression of *aprE,* as shown previously for the *motB* deletion (Cairns *et al.*, 2013). To inquire whether this increase depended on DegU, the *degU* gene was disrupted in the *hag* background. Although inactivation of *degU* did not affect the expression of *aprE* in the hag^+ strain, *aprE* expression in the *hag degU* strain reverted back to the wild-type level (Fig. 3), confirming that DegU mediates the increase in *aprE* transcription caused by deletion of *hag*.

High DegU-P in flagellar mutants represses the basal expression of *comK*

We next addressed which step in the *comK* signaling pathway is affected by the absence of flagella. Central to K-state decision-making is a positive feedback in which ComK directly activates its own promoter (van Sinderen & Venema, 1994, Maamar & Dubnau, 2005, Smits *et al.*, 2005, Gamba *et al.*, 2015). The decision to enter the K-state is governed by the basal level expression from P_{comK}, defined as expression in a *ΔcomK* mutant, in which the feedback is interrupted (Leisner *et al.*, 2007, Mirouze *et al.*, 2012). Basal expression normally rises during growth to a maximum at T_0 and then decreases. Because a threshold

basal concentration of ComK is needed to activate the positive feedback on P_{comK}, the probability that a cell will have enough ComK to induce transcription from P_{comK} increases and then decreases as cells enter the stationary phase of growth. This rise and fall in the basal rate of *comK* expression is due to the gradually increasing level of the phosphorylated master response regulator protein Spo0A-P during growth, because Spo0A-P activates and then represses *comK* transcription by directly binding to a series of operator sites in P*comK* (Mirouze *et al.*, 2012), Thus, within a temporal window of opportunity set by the rate of Spo0A-P accumulation, some cells in the population (~15% in the domesticated (laboratory) strains of *B. subtilis*) achieve a level of ComK sufficient to activate the positive feedback loop by binding to its own promoter. These cells switch to the K-state and become competent for transformation. Fig. 2B shows, using a P_{comK}-*luc* reporter in a *ΔcomK* strain, that the basal expression is lowered by the deletion of *hag*. This result suggests that the effect of the *hag* deletion is independent of ComK and its positive feedback loop. A *motB* mutant exhibits a similarly decreased basal level expression of *comK* (Fig. 2B). We conclude, based on the data in Figs. 1A and B, that when flagellar synthesis is perturbed, cells will have a lower chance to reach the threshold for ComK to activate its own expression and fewer cells will be able to enter the K-state and become competent for transformation. This result is consistent with the data in Fig. 2, which show a decreased frequency of K-state cells in the *fla/che* and *hag* deletants.

It has been shown that unphosphorylated DegU binds to the *comK* promoter (Hamoen *et al.*, 2000). This binding increases the affinity of ComK for its own promoter, thus lowering the threshold of ComK concentration needed to activate positive auto-regulation. To determine whether high DegU-P can inhibit the basal expression of *comK*, we used *degU32,* a $degU^{h}$ allele that increases the amount of DegU-P (Henner *et al.*, 1988, Dahl *et al.*, 1992). This mutation caused the reduced expression of P*comK-luc* in both wild-type and *ΔcomK* backgrounds (Fig. S1A and B), consistent with previous reports (Steinmetz *et al.*, 1976, Msadek *et al.*, 1990, Dahl *et al.*, 1992). It is not known if this negative effect is exerted directly on P_{comK}, but it is consistent with the possibility that the effect of flagellar mutations on K-state expression is mediated by DegU-P.

To further investigate the effects of *hag* inactivation on the basal expression of *comK* expression, we utilized two mutations that prevent the phosphorylation of DegU; a knockout of *degS* and a $degU^{D56N}$ mutation, which alters the site of phosphorylation (Msadek *et al.*, 1990, Dahl *et al.*, 1991). The P_{comK}-*luc* reporter was used in a *comK* mutant strain so that all the expression from this promoter reflects the basal expression (Fig. 4A). Importantly, both the D56N mutation and inactivation of *degS* bypass the effect of the *hag* deletion to levels of basal expression slightly higher than in the hag^{+} strain. This suggests that excess phosphorylation of DegU is responsible for the inhibition observed in the *hag* strain, while in the hag^{+} strain, the basal expression is probably limited by DegU-P. The *degS* and $DegU^{D56N}$ mutations similarly bypassed the deletion of *motB* (Fig. 4B).

It has been reported that the accumulation of DegU-P induces an increased level of Spo0A-P (Marlow *et al.*, 2014). Because excess Spo0A-P will repress the basal expression of *comK* by direct binding (Mirouze *et al.*, 2012), the effect of flagellar mutants could be mediated via an effect of DegU-P on the level of Spo0A-P. However, Fig. S2 shows that the deletion of

motB decreases the residual basal expression of *comK* in a *spo0A* deletion strain and that this decrease is suppressed by the DegU^{D56N} allele. Collectively, these findings show that a deletion of *motB* results in an increase in the level of DegU-P that represses the basal expression of *comK* and that this effect is probably not mediated by Spo0A-P. We do not know if DegU-P, like DegU, binds directly to the promoter region of *comK*.

K-state cells predominantly express low levels of DegU-P

To explore the relationship between DegU-P and the K-state on a single-cell level, we used a strain expressing a promoter fusion of *comK* to *cfp* as well as a *degU-yfp* promoter fusion placed downstream from the native *degU* gene (Fig. 5A). *degU* is transcribed from three promoters: P1 is in front of the *degSU* operon, while P2 and P3 transcribe *degU* (Fig. 5A). Importantly, DegU-P auto-regulates its own expression by positive feedback at P3 (Ogura & Tsukahara, 2010), so that a DegU-YFP fusion can be used as a readout to infer the level of DegU-P.

In this strain, the DegU-YFP signal was distributed heterogeneously across the population as reported previously (Veening *et al.*, 2008) (Fig. 5B, top row of images). ComK expression was observed to be negatively correlated with DegU-YFP expression, consistent with a role for DegU-P in down-regulation of the K-state. In this strain 3.8 % of the cells were scored visually as high expressing for YFP. Inactivation of *hag* resulted in an increase in the percentage of high YFP-expressing cells to 39 % (Fig. 5B, bottom row). At least 2000 cells were scored for each strain. This increase can be explained by autoregulation at P3. The activation of DegU phosphorylation caused by interference with flagellar function leads to an amount of DegU-P that exceeds the threshold for auto-activation in many cells. This would imply that the positive auto-regulation at the P3 promoter is at least partly responsible for the heterogeneous expression of DegU. As expected, the frequency of K-state cells in the *Δhag* population is lower than in the wild-type background, consistent with Fig. 2. These single cell data lead to two important conclusions. First, as predicted from the ensemble measurements transitions to the K-state occur preferentially in cells with low levels of DegU-P. Second, the elimination of *hag* causes an increase in DegU-P and a decrease in the frequency of K-state cells.

The hag strain has functional motors

What is the initial signal that leads to suppression of the accumulation of DegU-P? We can consider three possibilities for this primary signal; rotation, proton flux and viscous load on the flagellar filament. In their important study, Cairns *et al.* (2013) postulated that restriction of flagellar rotation or possibly of proton flux could activate the DegS-DegU signal transduction system. In support of these suggestions, a mutation in the conserved aspartate of MotB, essential for protonation and torque generation phenocopies the *motB* deletion. However, as noted above, if the primary signal is rotation or proton flux, it is not immediately obvious why a *hag* mutation would have the same phenotype as a *motB* knockout. It is known that in *E. coli*, elimination of the filament leaves intact hooks that still rotate driven by ion flux, whereas the *motB* mutant flagella would rotate only due to Brownian motion (Suzuki & Komeda, 1981, Yuan & Berg, 2008). If the motor continues to function in *hag* deletions in *B. subtilis* as in *E. coli*, it would support a role for viscous load

in generating the signal. However, if the signal strength is determined by the sum of the loads experienced by all the flagella in a cell, it is important to determine if the numbers of hooks, representative of the total number of basal bodies per cell, are the same in the wild-type and the *hag* mutant strains. To enable staining of hooks, we genetically altered the hook protein FlgE, by insertion of a cysteine (T123C) as previously described by Courtney *et al.* (2012) and swapped the mutation into the native locus by allelic exchange. The $flgE^{T123C}$ allele was swapped into the native locus and hooks were fluorescently labeled and counted in the wild-type and the *hag* mutant strains (Fig. 6). The average number of hooks was calculated in relation to the cell length because hook numbers increase with increasing cell length (Guttenplan *et al.*, 2013) (Fig. 6B and C). *hag* cells synthesized an average of 7 hooks per cell close to the number for the wild-type. Like the wild-type, the number of hooks appear to increase proportionally with cell length in the *hag* mutant.

To test motor functions in the *hag* strain, hook rotation was compared in wild-type and *hag* strains. To enable tethering of cells to a surface, we used the genetically altered hook protein $FlgE^{T123C}$. Swim assays confirmed the wild-type function of the mutated *flgE* allele (data not shown). Finally, a *hag* deletion was inserted into this $flgE^{T123C}$ background. Tethered cell assays were carried out on *hag* and wild-type cells attached to maleimide-coated surfaces as previously described (Blair *et al.*, 2008). Cell rotation was digitally recorded over a time period up to 100s and quantitatively analyzed using ImageJ and Matlab codes (Lele *et al.*, 2013). Motors in the *hag* deletion strain were functional; cells were observed to tether and rotate in a manner similar to motors in the wild-type strain (Fig. 7, Movies S1, S2). The average motor speed in the *hag* knockout strain was 0.7 +/− 0.2 Hz and the average torque was 341 +/− 68 pN-nm. The average motor speed in the wild-type cells was 0.8 +/− 0.2 Hz and the average torque was 353 +/− 117 (Table 2). These data suggest that flagellar motors in the *hag* knockouts and the wild type strains generate similar torque and that these strains contain similar numbers of basal bodies, suggesting that proton flow or rotation may not be the primary signals. We propose that the primary signal is load, sensed by helical filaments rotating in viscous media.

Straight filaments actively rotate and cause an increase in DegU-P levels

The load on a straight filament is lower than that on a helical flagellum rotating with the same angular velocity. To test whether the signal affecting the K-state is generated by load, we used a Hag^{A233V} substitution that results in straight filaments (Martinez *et al.*, 1968). This substitution was inserted into the *hag* gene and swapped into the native locus. To enable visualization of the flagella by Alexa488-maleimide labeling, a T209C mutation was also introduced (Blair *et al.*, 2008). The non-motile phenotype of this strain, previously described by (Martinez *et al.*, 1968), was confirmed on a swim agar plate (Fig. 8A). Wild-type and straight flagella stained with the fluorescent dye are shown in Fig. 8B, verifying the straight morphology of the mutant flagella.

The levels of DegU-P were inferred in the hag^{A233V} strain, by testing the transcription of *comK* and *aprE* (Fig. 8C and D). *comK* expression decreased, whereas *aprE* expression increased in the hag^{A233V} strain compared to wild-type. Thus, the results obtained for hag^{A233V} resemble those of the *hag* and *motB* deletions for DegU-P dependent gene

expression. Furthermore, a bypass experiment with the non-phosphorylatable *degU*^{D56N} allele confirmed that DegU-P is needed to activate *aprE* expression in the *hag*^{A233V} strain (Fig. 8D). These results show that the straight filament mutant produces high DegU-P and consequently lowers K-state expression, consistent with the hypothesis that the cells sense viscous drag to regulate DegU phosphorylation.

To determine whether the straight filament strain has functional motors, tethering experiments were performed, as described above for the *hag* mutant. Motor speeds, shown in Fig. 7, reveal that the straight filaments rotate and that functional motors are assembled (see also Movie S3). The average motor speed in the straight filament mutant was 0.4 +/− 0.1 Hz and the average torque was 248 +/− 38 pN-nm (Table 2). All measurements were at high viscous loads since the tethered cell represents a considerable load. Cells carrying the *hag*^{A233V} allele synthesized an average of 7.5 hooks per cells, close to the result for the wild-type (Fig. 6). No significant differences were observed between the *hag*^{A233V} mutant and wild-type in the cell length/hook number correlation (Fig. 6B and C). We conclude from these data, that disruption of motor functions in the straight flagella mutant is not the reason for low K-state expression and that the signal for K-state regulation is viscous drag on the flagellar filament.

Discussion

Our observations indicated a reduction in the K-state transition probability when the entire *fla/che* operon was deleted. Data also suggested that K-state cells carried lower levels of DegU-P. In a *hag* deletion strain and in a straight filament mutant, the normal DegU-P-suppressing signal was abrogated and DegU-P was elevated. Experiments confirmed that the flagellar motors were functional in these mutants. Considering that flagellar hooks spin at much higher speeds accompanied by a significant proton flux (Yuan & Berg, 2008), it is unlikely that the elevation in DegU-P is due to a cessation in either motor-rotation or the flux. Instead, given that the viscous loads in the two mutants are lower compared to the loads on motors in the wild type, it appears that motor operation at higher loads is necessary to suppress DegU-P. Presumably, the loads encountered by motors in freely swimming wild type cells are adequate for the suppression of DegU-P and any reduction in the load increases DegU-P. Our data further suggest that high DegU-P levels reduce the basal expression of *comK*, ultimately decreasing the number of cells in a population that exceed a threshold needed to activate positive auto-regulation at P_{comK}. These observations together strongly support a heuristic model in which the viscous drag on flagellar filaments mediates transition to the K-state.

We do not know if the phosphorylated protein binds directly to repress the basal expression of *comK*. In addition to ComK and DegU, it is known that AbrB, Rok and CodY bind to P*comK* (Hamoen *et al.*, 2003, Smits *et al.*, 2007) and it is possible that DegU-P acts via an effect on one of these proteins or in some other manner. Unphosphorylated DegU helps ComK bind to its own promoter, thereby activating positive auto-regulation (Hamoen *et al.*, 2000). However, it is unlikely that the depletion of DegU, due to increased phosphorylation, inhibits K-state expression. If DegU were to be depleted considerably due to phosphorylation, it would likely increase the level of ComK required to initiate auto-

regulation rather than lowering the basal expression. High Spo0A-P is known to repress the basal expression from P*comK* (Mirouze *et al.*, 2012) and it has been reported that elevated DegU-P increases the concentration of Spo0A-P (Marlow *et al.*, 2014) However, our results show that DegU-P is able to lower the residual basal expression in a *spo0A* knockout strain, making it less plausible that DegU-P action on P*comK* is mediated by Spo0A-P.

The number of stator-units bound to individual flagellar motors increases with viscous loads (Lele *et al.*, 2013, Tipping *et al.*, 2013). Our recent work suggested that this likely occurs due to a load-induced increase in the torque delivered by individual units (Chawla *et al.,* Sci Rep, in press). It is possible then, that the modulation of stator-assembly or the torque by the viscous load facilitates transitions to the K-state, Stalling of flagellar motors by locking filaments with anti-Hag antibodies was observed to elevate DegU-P levels (Cairns *et al.*, 2013). This appears to be at odds with the proposed mechanism since mechanical stalling results in maximum loads on individual motors in *E. coli* (Berry & Berg, 1997). However, it might be that the treatment with antibodies or motor-stall causes the dissociation of stators in *B. subtilis*, leading to a concomitant increase in the level of DegU-P. Although our study has focused on the regulation of the K-state by flagellar motors, it is tempting to suggest that the viscous load on the motor also regulates other forms of gene expression, such as the production of poly-γ-glutamate, exoprotease and biofilm formation (Osera *et al.*, 2009, Cairns *et al.*, 2013, Chan *et al.*, 2014). Indeed, DegU directly or indirectly regulates well over 150 genes (Ogura *et al.*, 2001, Mader *et al.*, 2002, Kobayashi, 2007).

Among the most interesting unanswered questions concern the biological roles of this signal transduction mechanism. Dynamic signaling by flagellar load may occur during switching between motile and sessile states in planktonic cells, when cells encounter a surface and initiate the formation of biofilms and during swarming, when viscous drag is likely to be greater than in free-swimming cells.

Experimental procedures

Strains and growth conditions

All strains are listed in Table S1. The *B. subtilis* strains used in this work are derived from the laboratory wild type strain IS75, a derivative of strain 168, or the undomesticated strain NCIB3610Δ*comI*. The *comI* mutation abolishes ComI activity (Konkol *et al.*, 2013), removing a block in DNA uptake. Constructs were introduced into IS75 by transformation (Albano *et al.*, 1987) and into NCIB3610 by transduction using bacteriophage SPP1 (Cozy & Kearns, 2010). Bacterial growth was at 37°C. Antibiotic selections were carried out on Luria Broth (LB) agar plates (10 g/L Tryptone, 5 g/L Yeast Extract and 5 g/L NaCl) containing ampicillin (100 μg ml^{-1}), spectinomycin (100 μg ml^{-1}), erythromycin (5 μg ml^{-1}), kanamycin (5 μg ml^{-1}), tetracycline (25 μg ml^{-1}) or chloramphenicol (5 μg ml^{-1}). In some cases selection was for erythromycin (1 μg ml^{-1}) plus lincomycin (20 μg ml^{-1}). Solid media were solidified by the addition of 1.5% agar. Transformation frequencies were determined using genomic DNA isolated from a leucine prototroph. Isopropyl beta-D-thiogalactopyranoside (IPTG, Sigma) was added to the medium at the indicated concentrations when appropriate.

Strain construction

To construct the following point mutations: *degU*^{D56N}, *hag*^{T209C}, *hag*^{A233V}, *hag*$^{T209C/A233V}$ and *flgE*^{T123C} at their native loci, we used the pMiniMAD2 cloning strategy, as described previously (Cozy & Kearns, 2010, Mukherjee *et al.*, 2013). Plasmids are listed in Table S2.

All oligonucleotides were provided by Eton Biosciences (Union, NJ) and are listed in Table S3. All plasmid constructs and all resulting *Bacillus* strains were confirmed by sequencing performed by Eton Biosciences. A fragment containing the *degU*^{D56N} mutation was amplified from genomic DNA containing the *degU*^{D56N} mutation (Msadek *et al.*, 1990) using the primers *degU*fwd and CD47-*degU*rev and cloned into the *Hind*III and *Kpn*I sites on plasmid pMiniMAD2. The resulting plasmid, pMiniMAD2-*degU*^{D56N} (pED1839), was used to create the strain BD7394.

A fragment containing the *hag* open reading frame was amplified from IS75 genomic DNA by using the primers CD60-*hag*fwd and CD61-*hag*rev and cloned into the *Bam*HI site on plasmid pMiniMAD2 using the In-Fusion HD cloning kit (Clontech). The resulting plasmid pED1933 was mutagenized using the Change-IT multiple mutation site-directed mutagenesis kit (Affymetrix), per the manufacturer's instructions and the primers CD62-*hagA233V* and CD78-*hagT209C*, to construct plasmids with the following pointmutations in *hag*: pED1907 (*hag*^{A233V}), pED1927 (*hag*^{T209C}) and pED1925 (*hag*$^{A233V\text{-}T209C}$). The plasmids were used to transform IS75 to create the strains BD7599 (*hag*^{A233V}), BD7816 (*hag*^{T209C}) and BD7757 (*hag*$^{A233V\text{-}T209C}$).

To construct the *flgE*^{T123C} allele, a fragment was amplified from genomic DNA containing the *flgE*^{T123C} mutation using the primers CD126A-*flgE*fwd and CD127A-*flgE*rev and cloned into the *Bam*HI site on plasmid pMiniMAD2 as described above. The plasmid pMiniMAD2-*flgE*^{T123C} (pED2004) was used to create BD8207.

To create a transcriptional promoter fusion of *degU* to mYpet (yellow fluorescent protein, Ohashi *et al.* (2007)), the *mYpet* coding sequence isolated from pDP429 via a *Sal*I and *Sph*I digest and a DNA fragment encoding the C-terminal portions of *degU* amplified with CD149-*degU-yfp*fwd and CD150-*degU-yfp*rev were cloned into the *EcoR*I and *Sal*I sites of the vector pUS19 (Benson & Haldenwang, 1993). The resulting plasmid pED2117 was transformed into *B. subtilis* to create a transcriptional promoter fusion of P*degU* to the m*Ypet* gene which has its own ribosomal binding site (BD8556).

Motility assay

Swimming analysis were performed as described before (Guttenplan *et al.*, 2013). Swim agar plates containing 25 ml of LB fortified with 0.3% Bacto agar were prepared the night before use and each plate was toothpick inoculated from an overnight colony and scored for motility after 18h at 30°C.

Microscopy

For P*comG-yfp* and *degU-yfp* P*comK-cfp* microscopy, cells were grown at 37°C in competence media until they reached the maximum of competence expression at T_2 (2h after transition from exponential to stationary phase of growth). One microliter of the cell culture

was spotted on an agarose pad (1% agarose made up in 0.5 x TAE buffer). Cells were imaged on an upright Nikon Eclipse 90i microscope outfitted with an Orca ER Digital Camera (Hamamatsu) with a Nikon Tirf 1.45 NA Plan Neoflur 100 oil immersion objective. Semrock Optical filter sets were used for fluorescence detection. The Volocity software package 6.3 was used for image acquisition.

For fluorescent microscopy of flagella filaments, cells were grown at 37°C in LB broth until they reached an OD_{600} of 0.5–0.8. 1 ml of broth culture was harvested and resuspended in 50 μl of PBS containing 5 μg/ml Alexa Fluor 488 C5 maleimide (Molecular Probes), and incubated for 5 min at room temperature. Cells were then washed with 1 ml of PBS and resuspended to an OD_{600} of 10. Samples were observed by spotting 1 ul of the suspension on an agarose pad (see above). Images were collected using a Nikon Eclipse Ti microscope equipped with an Orca Flash 4.0 Digital camera (Hamamatsu) with a Nikon TIRF 1.45 NA Plan Neoflur 100 oil immersion objective. NIS-Elements AR (v 4.40, Nikon) software was used for image acquisition and data analysis.

For fluorescent microscopy of flagella hooks, cells were grown at 37°C in LB broth until they reached an OD600 of 0.5–0.8. 1.0 ml of broth culture was harvested and resuspended in 30 μl of PBS containing 5μg/ml Alexa Fluor 488 C5 maleimide (Molecular Probes), and incubated for 5 min at room temperature. Cells were then washed with 1 ml of PBS, pelleted, and supernatant removed. Membranes were stained by resuspension in 30 μl of PBS containing 5 μg/ml FM4-64 and incubated for 5 min at room temperature. Cells were washed in 1 ml of PBS, and pelleted again. Samples were finally resuspended to an OD_{600} of 10 in PBS. Samples were observed by spotting 4 μl of the suspension on a glass microscope slide and immobilized with a poly-L-lysine-treated glass coverslip.

Conventional fluorescence microscopy was performed with a Nikon 80i microscope with a phase contrast objective Nikon Plan Apo 100X and an Excite 120 metal halide lamp. FM4-64 membrane stains were visualized with a C-FL HYQ Texas Red Filter Cube (excitation filter 532–587 nm, barrier filter 590 nm). Alexa Fluor 488 C5 maleimide fluorescent signals were visualized using a C-FL HYQ FITC Filter Cube (FITC, excitation filter 460–500 nm, barrier filter 515–550 nm). Images were captured with a Photometrics Coolsnap HQ2 camera in black and white, false colored, and superimposed using Metamorph image software.

Super Resolution fluorescence microscopy was performed using the structured illumination OMX 3D-SIM Super Resolution system at Indiana University Bloomington Light Microscopy Imaging Center. Super Resolution microscopy was performed using a 1.4NA Olympus 100x oil objective. FM4-64 was visualized using laser line 561nm and emission filter 609–654nm, and Alexa Fluor 488 was visualized using laser line 488nm and emission filter 500–550 nm. Images were captured by Photometrics Cascade II EMCCD camera, and processed by SoftWoRx software (Applied Precision).

To count hooks, images reconstructed with SoftWoRx were processed in Imaris (Bitplane) to measure cell length and determine the number of $FlgE^{T123C}$ foci on the surface of each cell. Cell length was measured by hand using the ‘Slice’ measurement tool. The ‘Spots’ feature

labelled each $FlgE^{T123C}$ foci by identifying spots of 0.1 μM in the 488 wavelength range. We then verified by eye that the labelling identified bona fide foci on the cell surface. Number of foci was then recorded and plotted against cell length.

Tethering

Overnight cultures were diluted in fresh TB (10 g/L tryptone; 5 g/L NaCl) at 30°C and grown to an OD_{600} of 0.5–0.6. Cells were washed twice in motility buffer containing lactate (0.055 M NaCl, 10 mM EDTA, 10 mM potassium phosphate, pH 7.0) and sheared 70 times to shorten the filaments (Ford *et al.*, 2017). These strains carried cysteine groups in the flagellin or hook proteins ($hag^{T209C}/flgET^{123C}$) in order to facilitate tethering to maleimide-coated coverslips (MicroSurfaces, Inc.). Cells were allowed to tether for 10 minutes and observed with a 20 X objective on an inverted microscope (Nikon Ti-E). Cell-geometries and rotational-speeds were quantitatively tracked with custom-written MATLAB codes (Lele *et al.*, 2016).

Luciferase assays

For the detection of luciferase activity, strains were first grown in LB medium to an OD_{600} of 2. Cells were then centrifuged and resuspended in fresh competence medium (Albano *et al.*, 1987), adjusting all the cultures to an OD_{600} of 2. These pre-cultures were then diluted 20-fold in fresh competence medium and 200 μl was distributed in each of two wells in a 96-well black plate (Corning Incorporated Costar®). 10 μl of luciferin was added to each well to reach a final concentration of 1.5 mg/ml (4.7 mM). The cultures were incubated at 37°C with agitation in a PerkinElmer Envision 2104 Multilabel Reader equipped with an enhanced sensitivity photomultiplier for luminometry. The temperature of the clear plastic lid was maintained at 38°C to avoid condensation. Relative Luminescence Units (RLU) and OD_{600} were measured at 1 min intervals after two 30 second shaking steps. The data were processed using a script written in MATLAB, exported to Excel and plotted as RLU/OD_{600} versus time from the beginning of growth.

Supplementary Material

Refer to Web version on PubMed Central for supplementary material.

Acknowledgments

This work was supported by NIH grant GM057720 (DD), NIH GM093030 to DBK and by funds from the Texas A&M Engineering Experiment Station (PL). We thank K. Lemon and A. Grossman for the gift of the pKL184 plasmid.

References

Adler J. Chemotaxis in bacteria. Annu Rev Biochem. 1975; 44:341–356. [PubMed: 1094913]

Albano M, Hahn J, Dubnau D. Expression of competence genes in Bacillus subtilis. J Bacteriol. 1987; 169:3110–3117. [PubMed: 3110135]

Armitage JP. Bacterial motility and chemotaxis. Sci Prog. 1992; 76:451–477. [PubMed: 1364581]

Belas R. Biofilms, flagella, and mechanosensing of surfaces by bacteria. Trends Microbiol. 2014; 22:517–527. [PubMed: 24894628]

Belas R, Simon M, Silverman M. Regulation of lateral flagella gene transcription in Vibrio parahaemolyticus. J Bacteriol. 1986; 167:210–218. [PubMed: 3013835]

Benson AK, Haldenwang WG. Regulation of sigma B levels and activity in Bacillus subtilis. J Bacteriol. 1993; 175:2347–2356. [PubMed: 8468294]

Berg HC. The rotary motor of bacterial flagella. Annu Rev Biochem. 2003; 72:19–54. [PubMed: 12500982]

Berg HC, Brown DA. Chemotaxis in Escherichia coli analysed by three-dimensional tracking. Nature. 1972; 239:500–504. [PubMed: 4563019]

Berka RM, Hahn J, Albano M, Draskovic I, Persuh M, Cui X, Sloma A, Widner W, Dubnau D. Microarray analysis of the Bacillus subtilis K-state: genome-wide expression changes dependent on ComK. Mol Microbiol. 2002; 43:1331–1345. [PubMed: 11918817]

Berry RM, Berg HC. Absence of a barrier to backwards rotation of the bacterial flagellar motor demonstrated with optical tweezers. Proc Natl Acad Sci U S A. 1997; 94:14433–14437. [PubMed: 9405630]

Blair KM, Turner L, Winkelman JT, Berg HC, Kearns DB. A molecular clutch disables flagella in the Bacillus subtilis biofilm. Science. 2008; 320:1636–1638. [PubMed: 18566286]

Block SM, Berg HC. Successive incorporation of force-generating units in the bacterial rotary motor. Nature. 1984; 309:470–472. [PubMed: 6374467]

Caiazza NC, Merritt JH, Brothers KM, O'Toole GA. Inverse regulation of biofilm formation and swarming motility by Pseudomonas aeruginosa PA14. J Bacteriol. 2007; 189:3603–3612. [PubMed: 17337585]

Caiazza NC, O'Toole GA. SadB is required for the transition from reversible to irreversible attachment during biofilm formation by Pseudomonas aeruginosa PA14. J Bacteriol. 2004; 186:4476–4485. [PubMed: 15231779]

Cairns LS V, Marlow L, Bissett E, Ostrowski A, Stanley-Wall NR. A mechanical signal transmitted by the flagellum controls signalling in *Bacillus subtilis*. Mol Microbiol. 2013; 90:6–21. [PubMed: 23888912]

Chan JM, Guttenplan SB, Kearns DB. Defects in the flagellar motor increase synthesis of poly-gamma-glutamate in Bacillus subtilis. J Bacteriol. 2014; 196:740–753. [PubMed: 24296669]

Che YS, Nakamura S, Morimoto YV, Kami-Ike N, Namba K, Minamino T. Load-sensitive coupling of proton translocation and torque generation in the bacterial flagellar motor. Mol Microbiol. 2014; 91:175–184. [PubMed: 24255940]

Chevance FF, Hughes KT. Coordinating assembly of a bacterial macromolecular machine. Nat Rev Microbiol. 2008; 6:455–465. [PubMed: 18483484]

Courtney CR, Cozy LM, Kearns DB. Molecular characterization of the flagellar hook in Bacillus subtilis. J Bacteriol. 2012; 194:4619–4629. [PubMed: 22730131]

Cozy LM, Kearns DB. Gene position in a long operon governs motility development in Bacillus subtilis. Mol Microbiol. 2010; 76:273–285. [PubMed: 20233303]

Dahl MK, Msadek T, Kunst F, Rapoport G. Mutational analysis of the Bacillus subtilis DegU regulator and its phosphorylation by the DegS protein kinase. J Bacteriol. 1991; 173:2539–2547. [PubMed: 1901568]

Dahl MK, Msadek T, Kunst F, Rapoport G. The phosphorylation state of the DegU response regulator acts as a molecular switch allowing either degradative enzyme synthesis or expression of genetic competence in Bacillus subtilis. J Biol Chem. 1992; 267:14509–14514. [PubMed: 1321152]

Ellison C, Brun YV. Mechanosensing: a regulation sensation. Curr Biol. 2015; 25:R113–115. [PubMed: 25649820]

Ford KM, Chawla R, Lele PP. Biophysical Characterization of Flagellar Motor Functions. J Vis Exp. 2017

Gamba P, Jonker MJ, Hamoen LW. A Novel Feedback Loop That Controls Bimodal Expression of Genetic Competence. PLoS Genet. 2015; 11:e1005047. [PubMed: 26110430]

Guttenplan SB, Blair KM, Kearns DB. The EpsE flagellar clutch is bifunctional and synergizes with EPS biosynthesis to promote Bacillus subtilis biofilm formation. PLoS Genet. 2010; 6:e1001243. [PubMed: 21170308]

Guttenplan SB, Shaw S, Kearns DB. The cell biology of peritrichous flagella in Bacillus subtilis. Mol Microbiol. 2013; 87:211–229. [PubMed: 23190039]

Hahn J, Tanner AW, Carabetta VJ, Cristea IM, Dubnau D. ComGA-RelA interaction and persistence in the Bacillus subtilis K-state. Mol Microbiol. 2015; 97:454–471. [PubMed: 25899641]

Hamoen LW, Smits WK, de Jong A, Holsappel S, Kuipers OP. Improving the predictive value of the competence transcription factor (ComK) binding site in Bacillus subtilis using a genomic approach. Nucleic Acids Res. 2002; 30:5517–5528. [PubMed: 12490720]

Hamoen LW, Van Werkhoven AF, Venema G, Dubnau D. The pleiotropic response regulator DegU functions as a priming protein in competence development in Bacillus subtilis. Proc Natl Acad Sci U S A. 2000; 97:9246–9251. [PubMed: 10908654]

Hamoen LW, Venema G, Kuipers OP. Controlling competence in Bacillus subtilis: shared use of regulators. Microbiology. 2003; 149:9–17. [PubMed: 12576575]

Henner DJ, Yang M, Ferrari E. Localization of Bacillus subtilis sacU(Hy) mutations to two linked genes with similarities to the conserved procaryotic family of two-component signalling systems. J Bacteriol. 1988; 170:5102–5109. [PubMed: 3141378]

Kobayashi K. Gradual activation of the response regulator DegU controls serial expression of genes for flagellum formation and biofilm formation in Bacillus subtilis. Mol Microbiol. 2007; 66:395–409. [PubMed: 17850253]

Kojima S, Blair DF. Conformational change in the stator of the bacterial flagellar motor. Biochemistry. 2001; 40:13041–13050. [PubMed: 11669642]

Kojima S, Blair DF. Solubilization and purification of the MotA/MotB complex of Escherichia coli. Biochemistry. 2004; 43:26–34. [PubMed: 14705928]

Konkol MA, Blair KM, Kearns DB. Plasmid-encoded ComI inhibits competence in the ancestral 3610 strain of Bacillus subtilis. J Bacteriol. 2013; 195:4085–4093. [PubMed: 23836866]

Leisner M, Stingl K, Radler JO, Maier B. Basal expression rate of comK sets a ‘switching-window’ into the K-state of Bacillus subtilis. Mol Microbiol. 2007; 63:1806–1816. [PubMed: 17367397]

Lele PP, Hosu BG, Berg HC. Dynamics of mechanosensing in the bacterial flagellar motor. Proc Natl Acad Sci U S A. 2013; 110:11839–11844. [PubMed: 23818629]

Lele PP, Roland T, Shrivastava A, Chen Y, Berg HC. The flagellar motor of Caulobacter crescentus generates more torque when a cell swims backward. Nat Phys. 2016; 12:175–178. [PubMed: 27499800]

Li G, Brown PJ, Tang JX, Xu J, Quardokus EM, Fuqua C, Brun YV. Surface contact stimulates the just-in-time deployment of bacterial adhesins. Mol Microbiol. 2012; 83:41–51. [PubMed: 22053824]

Maamar H, Dubnau D. Bistability in the Bacillus subtilis K-state (competence) system requires a positive feedback loop. Mol Microbiol. 2005; 56:615–624. [PubMed: 15819619]

Maamar H, Raj A, Dubnau D. Noise in gene expression determines cell fate in Bacillus subtilis. Science. 2007; 317:526–529. [PubMed: 17569828]

Mader U, Antelmann H, Buder T, Dahl MK, Hecker M, Homuth G. Bacillus subtilis functional genomics: genome-wide analysis of the DegS-DegU regulon by transcriptomics and proteomics. Mol Genet Genomics. 2002; 268:455–467. [PubMed: 12471443]

Marlow VL, Porter M, Hobley L, Kiley TB, Swedlow JR, Davidson FA, Stanley-Wall NR. Phosphorylated DegU manipulates cell fate differentiation in the Bacillus subtilis biofilm. J Bacteriol. 2014; 196:16–27. [PubMed: 24123822]

Marquez-Magana LM, Chamberlin MJ. Characterization of the sigD transcription unit of Bacillus subtilis. J Bacteriol. 1994; 176:2427–2434. [PubMed: 8157612]

Martinez RJ, Ichiki AT, Lundh NP, Tronick SR. A single amino acid substitution responsible for altered flagellar morphology. J Mol Biol. 1968; 34:559–564. [PubMed: 4999726]

McCarter L, Hilmen M, Silverman M. Flagellar dynamometer controls swarmer cell differentiation of V. parahaemolyticus. Cell. 1988; 54:345–351. [PubMed: 3396074]

Minamino T, Imada K, Namba K. Molecular motors of the bacterial flagella. Curr Opin Struct Biol. 2008; 18:693–701. [PubMed: 18848888]

Mirouze N, Desai Y, Raj A, Dubnau D. Spo0A~P imposes a temporal gate for the bimodal expression of competence in Bacillus subtilis. PLoS Genet. 2012; 8:e1002586. [PubMed: 22412392]

Msadek T, Kunst F, Henner D, Klier A, Rapoport G, Dedonder R. Signal transduction pathway controlling synthesis of a class of degradative enzymes in Bacillus subtilis: expression of the regulatory genes and analysis of mutations in degS and degU. J Bacteriol. 1990; 172:824–834. [PubMed: 1688843]

Mukherjee S, Babitzke P, Kearns DB. FliW and FliS function independently to control cytoplasmic flagellin levels in Bacillus subtilis. J Bacteriol. 2013; 195:297–306. [PubMed: 23144244]

Mukherjee S, Kearns DB. The structure and regulation of flagella in Bacillus subtilis. Annu Rev Genet. 2014; 48:319–340. [PubMed: 25251856]

Murray EJ, Kiley TB, Stanley-Wall NR. A pivotal role for the response regulator DegU in controlling multicellular behaviour. Microbiology. 2009; 155:1–8. [PubMed: 19118340]

Ogura M, Tsukahara K. Autoregulation of the Bacillus subtilis response regulator gene degU is coupled with the proteolysis of DegU-P by ClpCP. Mol Microbiol. 2010; 75:1244–1259. [PubMed: 20070525]

Ogura M, Yamaguchi H, Kobayashi K, Ogasawara N, Fujita Y, Tanaka T. Whole-genome analysis of genes regulated by the Bacillus subtilis competence transcription factor ComK. J Bacteriol. 2002; 184:2344–2351. [PubMed: 11948146]

Ogura M, Yamaguchi H, Yoshida K, Fujita Y, Tanaka T. DNA microarray analysis of Bacillus subtilis DegU, ComA and PhoP regulons: an approach to comprehensive analysis of B.subtilis two-component regulatory systems. Nucleic Acids Res. 2001; 29:3804–3813. [PubMed: 11557812]

Ohashi T, Galiacy SD, Briscoe G, Erickson HP. An experimental study of GFP-based FRET, with application to intrinsically unstructured proteins. Protein Sci. 2007; 16:1429–1438. [PubMed: 17586775]

Osera C, Amati G, Calvio C, Galizzi A. SwrAA activates poly-gamma-glutamate synthesis in addition to swarming in Bacillus subtilis. Microbiology. 2009; 155:2282–2287. [PubMed: 19389763]

Purcell EM. Life at low Reynolds number. American Journal of Physics. 1977; 45:3–11.

Smits WK, Eschevins CC, Susanna KA, Bron S, Kuipers OP, Hamoen LW. Stripping Bacillus: ComK auto-stimulation is responsible for the bistable response in competence development. Mol Microbiol. 2005; 56:604–614. [PubMed: 15819618]

Smits WK, Hoa TT, Hamoen LW, Kuipers OP, Dubnau D. Antirepression as a second mechanism of transcriptional activation by a minor groove binding protein. Mol Microbiol. 2007; 64:368–381. [PubMed: 17493123]

Steinmetz M, Kunst F, Dedonder R. Mapping of mutations affecting synthesis of exocellular enzymes in Bacillus subtilis. Identity of the sacUh, amyB and pap mutations. Mol Gen Genet. 1976; 148:281–285. [PubMed: 827683]

Suel GM, Garcia-Ojalvo J, Liberman LM, Elowitz MB. An excitable gene regulatory circuit induces transient cellular differentiation. Nature. 2006; 440:545–550. [PubMed: 16554821]

Suzuki T, Komeda Y. Incomplete flagellar structures in Escherichia coli mutants. J Bacteriol. 1981; 145:1036–1041. [PubMed: 7007337]

Tipping MJ, Delalez NJ, Lim R, Berry RM, Armitage JP. Load-dependent assembly of the bacterial flagellar motor. MBio. 2013:4.

Van Dellen KL, Houot L, Watnick PI. Genetic analysis of Vibrio cholerae monolayer formation reveals a key role for DeltaPsi in the transition to permanent attachment. J Bacteriol. 2008; 190:8185–8196. [PubMed: 18849423]

van Sinderen D, Luttinger A, Kong L, Dubnau D, Venema G, Hamoen L. comK encodes the competence transcription factor, the key regulatory protein for competence development in Bacillus subtilis. Mol Microbiol. 1995; 15:455–462. [PubMed: 7783616]

van Sinderen D, Venema G. comK acts as an autoregulatory control switch in the signal transduction route to competence in Bacillus subtilis. J Bacteriol. 1994; 176:5762–5770. [PubMed: 8083168]

Veening JW, Igoshin OA, Eijlander RT, Nijland R, Hamoen LW, Kuipers OP. Transient heterogeneity in extracellular protease production by Bacillus subtilis. Mol Syst Biol. 2008; 4:184. [PubMed: 18414485]

Verhamme DT, Kiley TB, Stanley-Wall NR. DegU co-ordinates multicellular behaviour exhibited by Bacillus subtilis. Mol Microbiol. 2007; 65:554–568. [PubMed: 17590234]

Yuan J, Berg HC. Resurrection of the flagellar rotary motor near zero load. Proc Natl Acad Sci U S A. 2008; 105:1182–1185. [PubMed: 18202173]

Zuberi AR, Ying CW, Weinreich MR, Ordal GW. Transcriptional organization of a cloned chemotaxis locus of Bacillus subtilis. J Bacteriol. 1990; 172:1870–1876. [PubMed: 2108125]

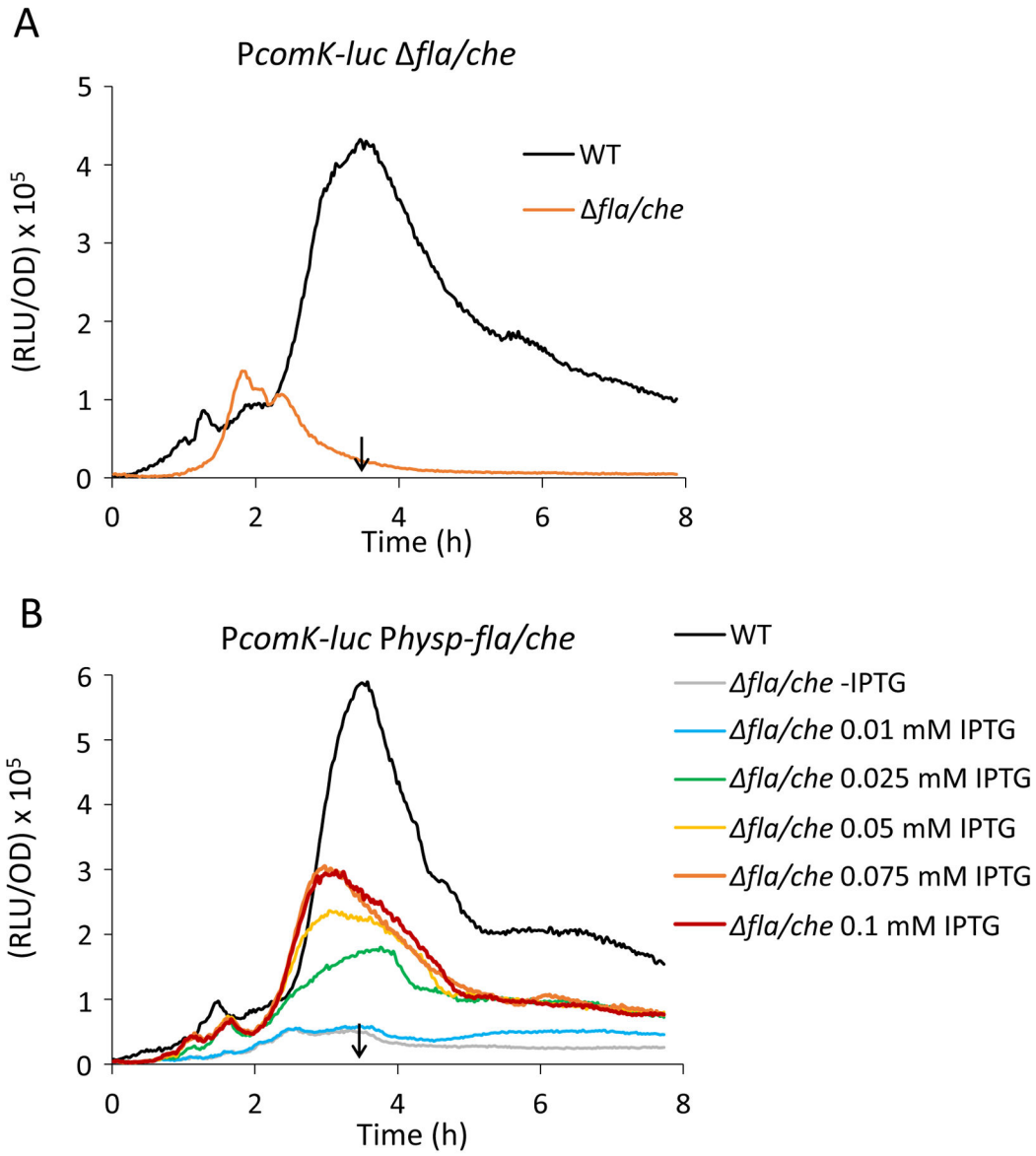

Figure 1.

Low *comK* expression in the absence of flagella synthesis. (A) The rate of *comK* expression is inhibited in the *fla/che* deletion strain (BD7763) compared to its isogenic wild-type equivalent (BD6439). (B) Dose-dependent suppression of *comK* expression by flagellar synthesis. Transcription rates from the P*comK-luc* reporter in a strain with an IPTG inducible *fla/che* operon in the native locus. Strain BD7695 (P*hysp-fla/che-operon PcomK-luc*) was grown in the absence and presence of different concentrations of IPTG (as indicated). P*comK-luc* expression in the wild-type (BD6439) is shown for comparison. All strains used for this experiment were built in the undomesticated background NCIB 3610. The vertical arrows in each panel point to the time of entry into stationary phase (T_0), determined from optical density measurements during growth in the plate reader.

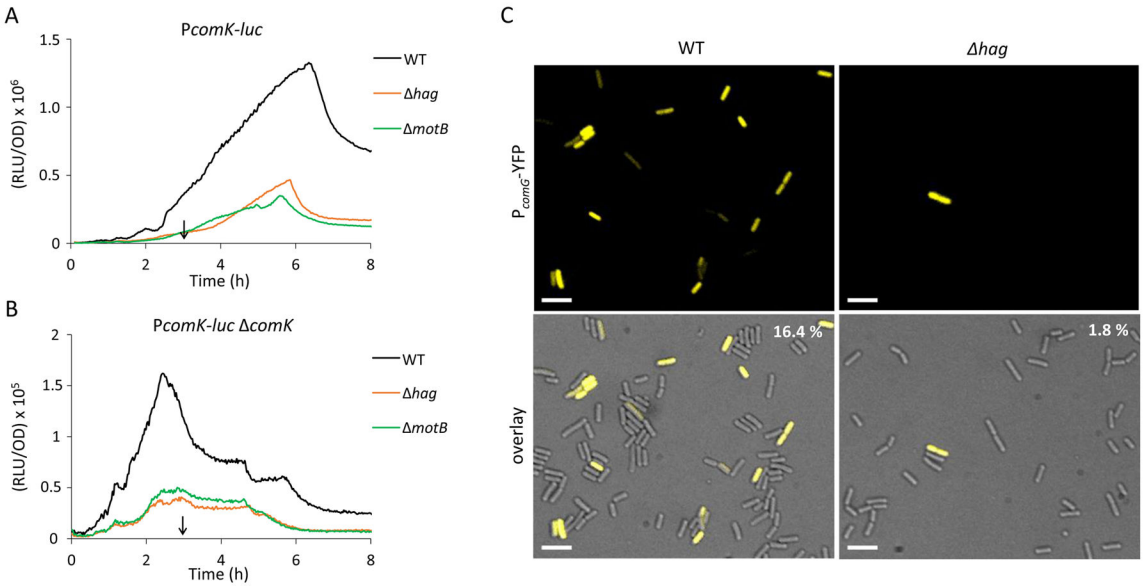

Figure 2.

Deletion of *hag* and *motB* lower the expression of *comK* and a *Δhag* mutation lowers the frequency of entry to the K-state. The effects of *hag* and *motB* knockouts on P*comK-luc* expression in the presence (A) or absence (B) of ComK are shown. The following strains were used in these experiments: wild-type P*comK-luc* (BD4773), *Δhag* P*comK-luc* (BD7636), *ΔmotB* P*comK-luc* (BD7466), *ΔcomK* P*comK-luc* (BD4893), *Δhag ΔcomK* P*comK-luc* (BD7261) and *ΔmotB ΔcomK* P*comK-luc* (BD7488). The expression profiles in A and B are plotted on different scales. The vertical arrows in panels A and B point to T_0. (C) Single-cell expression and microscopic enumeration of P*comG-yfp* expressing cells in *Δhag* (BD7262) and wild-type (BD5783) populations. The indicated strains were grown to the time of maximum K-state expression (T_2) and samples were taken for microscopy. Representative images are shown. In the upper right corner are the average percentages of K-state cells determined by counting at least 1000 cells for each strain, done in duplicate. Scale bar is 5μm.

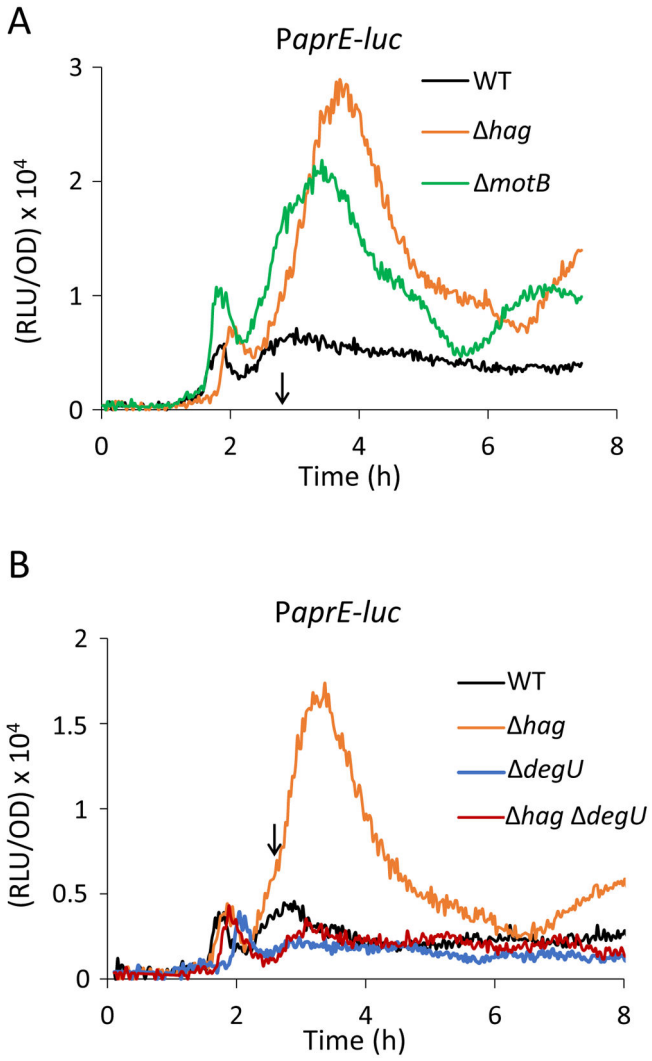

Figure 3.

DegU mediates the increase in *aprE* transcription caused by deletion of *hag*. (A) Increased expression of the P*aprE-luc* reporter in the *hag* and *motB* knock out strains. (B) *aprE* expression can be completely suppressed by a *degU* deletion in the *hag* background. The strains used were as follows: wild-type P*aprE-luc* (BD6904), *Δhag* P*aprE-luc* (BD7639), *ΔmotB* P*aprE-luc* (BD7719), *ΔdegU* P*aprE-luc* (BD7084) and *Δhag ΔdegU* P*aprE-luc* (BD7371). The vertical arrows in each panel point to T_0.

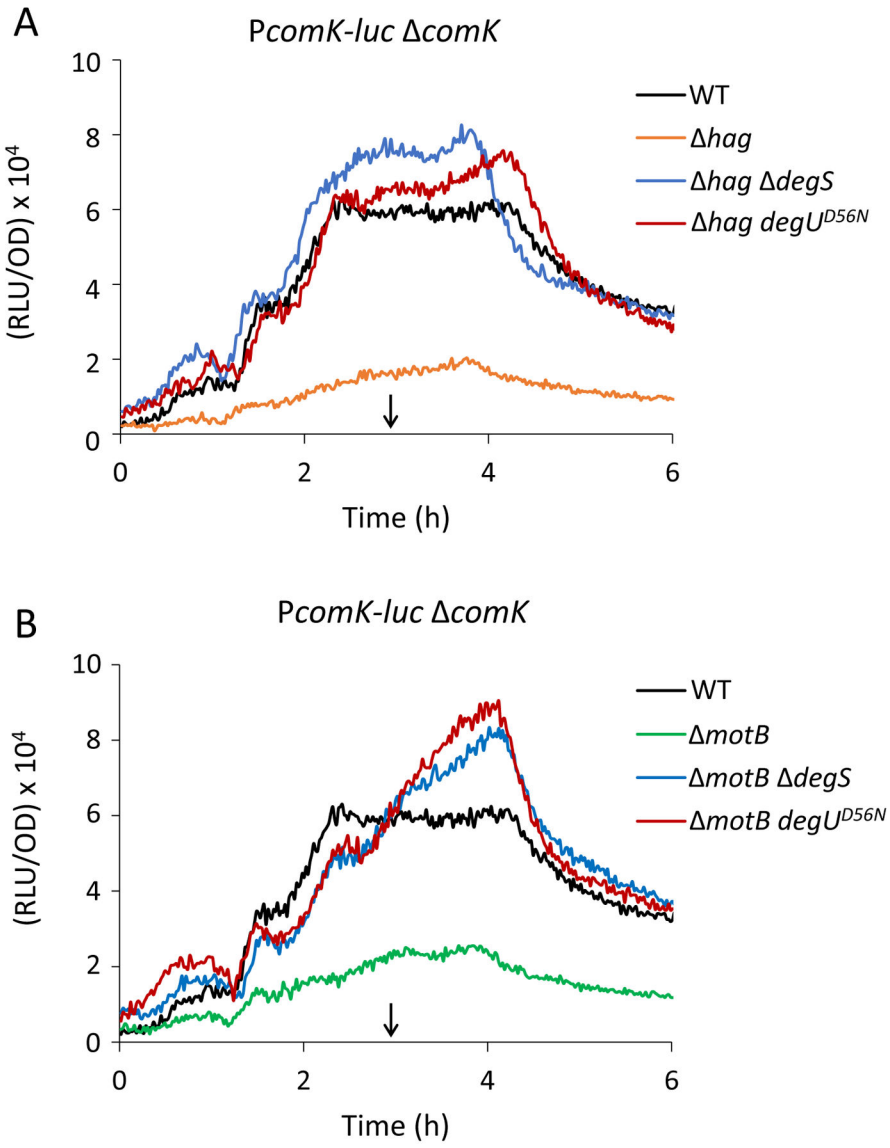

Figure 4.

DegU phosphorylation represses the basal expression of *comK* in *motB* and *hag* knockouts. The expression curves show P*comK-luc* expression in a *comK* deletion background. The *degU*^{D56N} allele as well as the *degS* deletion bypass *Δhag* (A) and *ΔmotB* (B) for expression from P*comK*. Strains used were as follows: *ΔcomK* P*comK-luc* (BD4893), *Δhag ΔcomK PcomK-luc* (BD7261), *ΔmotB ΔcomK* P*comK-luc* (BD7488), *Δhag ΔdegS ΔcomK PcomK-luc* (BD7491), *ΔmotB ΔdegS ΔcomK* P*comK-luc* (BD7490), *Δhag degU*^{D56N}*Δ comK PcomK-luc* (BD7475) and *ΔmotB degU*^{D56N} *ΔcomK* P*comK-luc* (BD7492). The vertical arrows point to T_0.

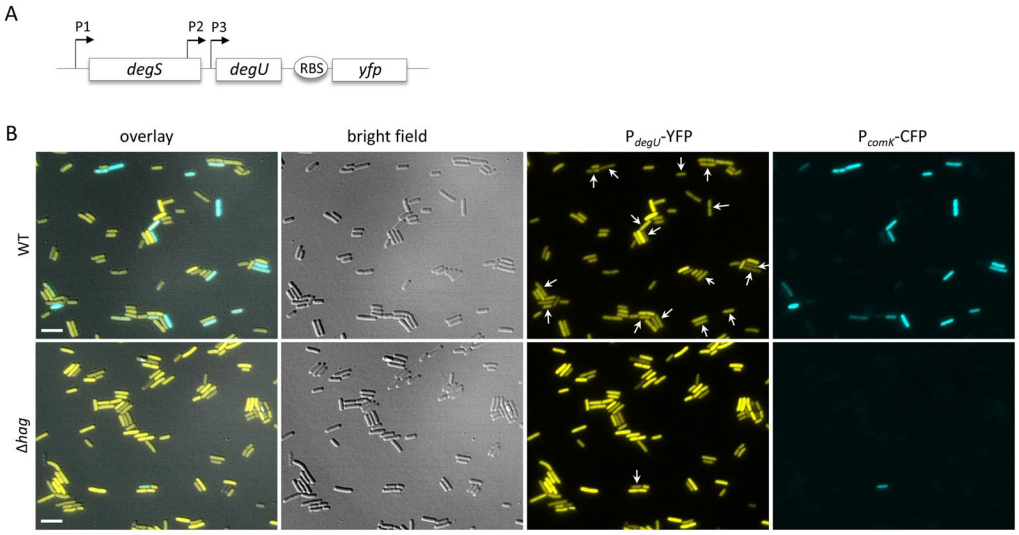

Figure 5.

K-state cells have low DegU-P. (A) The diagram explains the construct used for panel B. YFP with its own ribosomal binding site was placed downstream of the *degS degU* operon, so that it is expressed from the three native promoters. The P3 promoter is activated by DegU-P (Ogura & Tsukahara, 2010). This strain (BD8556) also carries P*comK-cfp* (blue) to monitor expression of the K-state. (B) The top row shows expression of YFP (yellow) and CFP (blue) in strain BD8556 while the bottom row shows expression from its isogenic equivalent (BD8557) that also carries a *hag* deletion. In the P_{degU}-YFP images, the *comK* expressing cells are indicated by arrows. In the *Δhag* strain, 39 % of the cells were scored visually as expressing high level of YFP, whereas in the wild-type strain shown in the top row, 3.8 % were high expressers. More than 2000 cells were scored for each strain. Cultures were grown to the time of maximum competence (T_2). Representative images are shown. Scale bar is 5 μm.

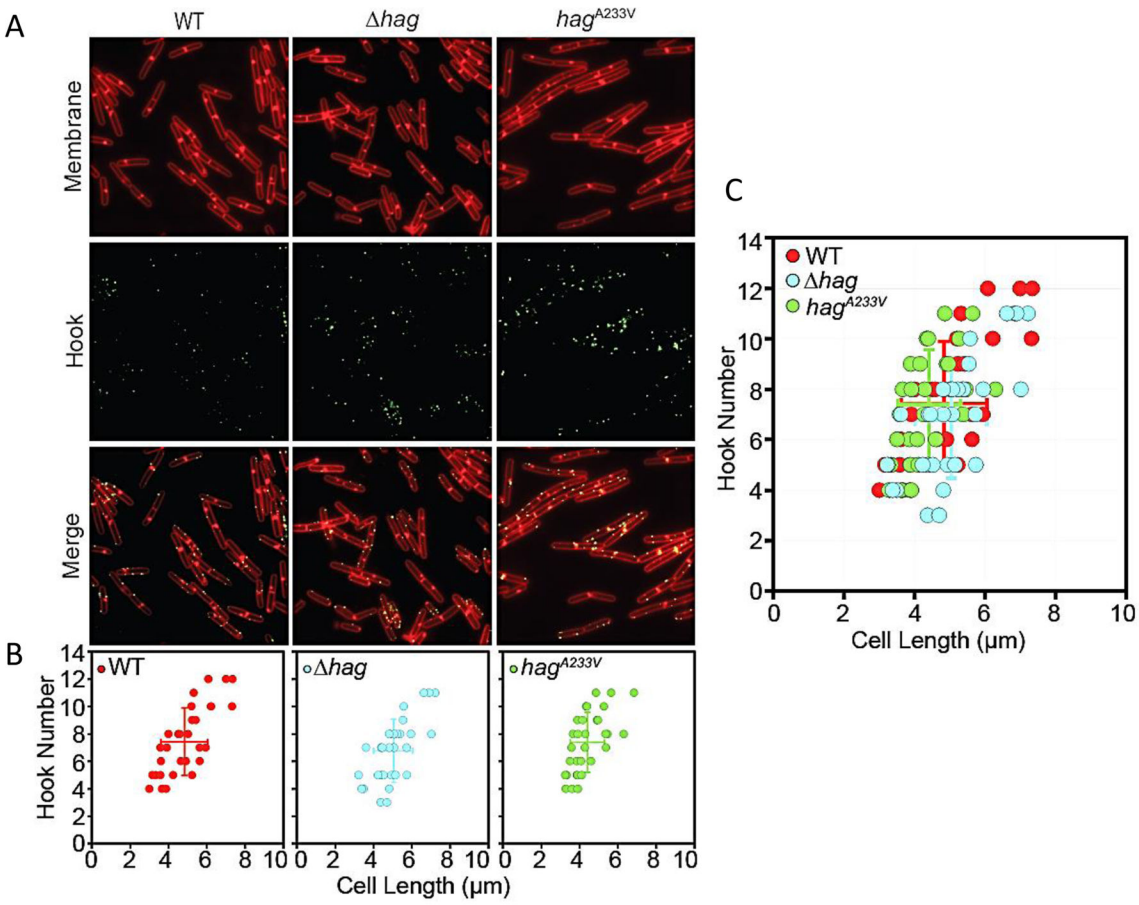

Figure 6.

Basal body numbers are unaltered in *Δhag* and *hag*^{A233V} mutants. (A) Fluorescence microscopy of strains with the indicated genotypes stained for membranes with FM4-64 (red) and flagellar hooks (green). The following strains were used: wild-type (DK3455), *Δhag* (BD8396) and *hag*^{A233V} (DK3456). (B) Graphical representation of flagellar hooks as determined by counting the number of FlgE^{T123C} puncta per cell per cell length using Imaris image analysis software. Individual cell data presented as a scatter plot. Average of length and spot number indicated as a larger solid dot with standard deviations that emerge from the solid dot as horizontal and vertical lines. N = 28 cells. Red symbols indicate wild-type (DK3455), blue symbols indicate *Δhag* (BD8396) and green symbols indicate *hag*^{A233V} (DK3456). (C) Overlay of hook scatter plots from (B).

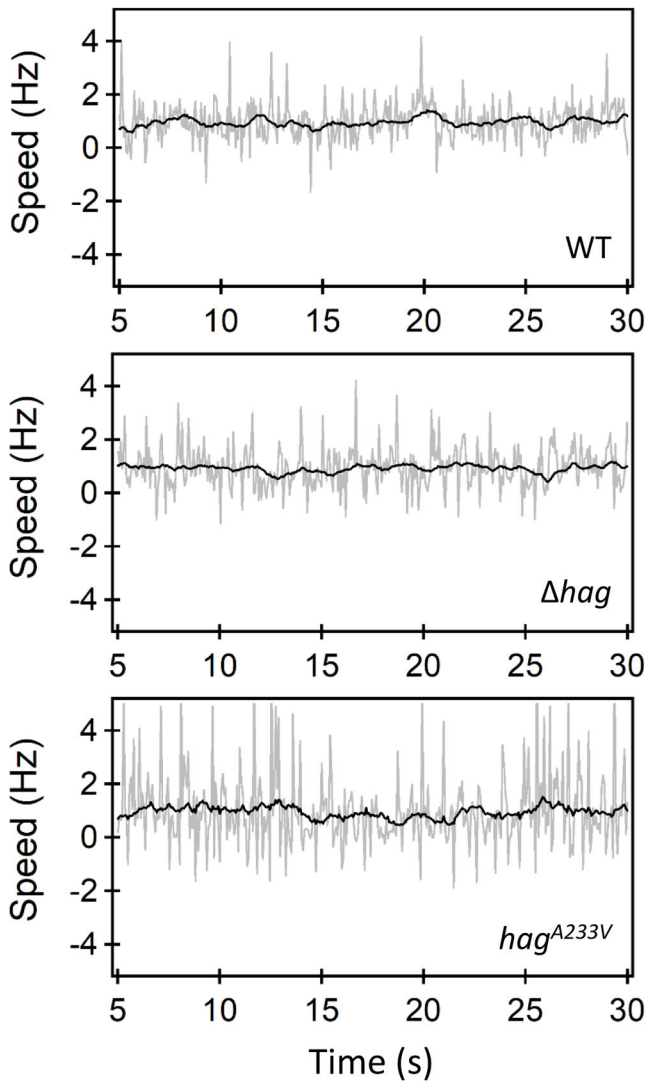

Figure 7.

A *hag* deletant and a straight filament mutant have functional motors. Rotational speeds of individual tethered cells belonging to the wild-type strain (top panel), the *Δhag* strain (middle panel) and the straight mutant (bottom panel) are indicated. The gray lines indicate raw data and the black curves represent filtered values. A majority of the cells predominantly rotated in the CCW direction (positive speeds). A small fraction (< 10%) of the cells exhibited CW rotation. Strains used for this experiment were: wild-type $flgE^{T123C}$ (BD8207), $\Delta hag\ flgE^{T123C}$ (BD8263) and $hag^{A233V\text{-}T209C}$ (BD7757).

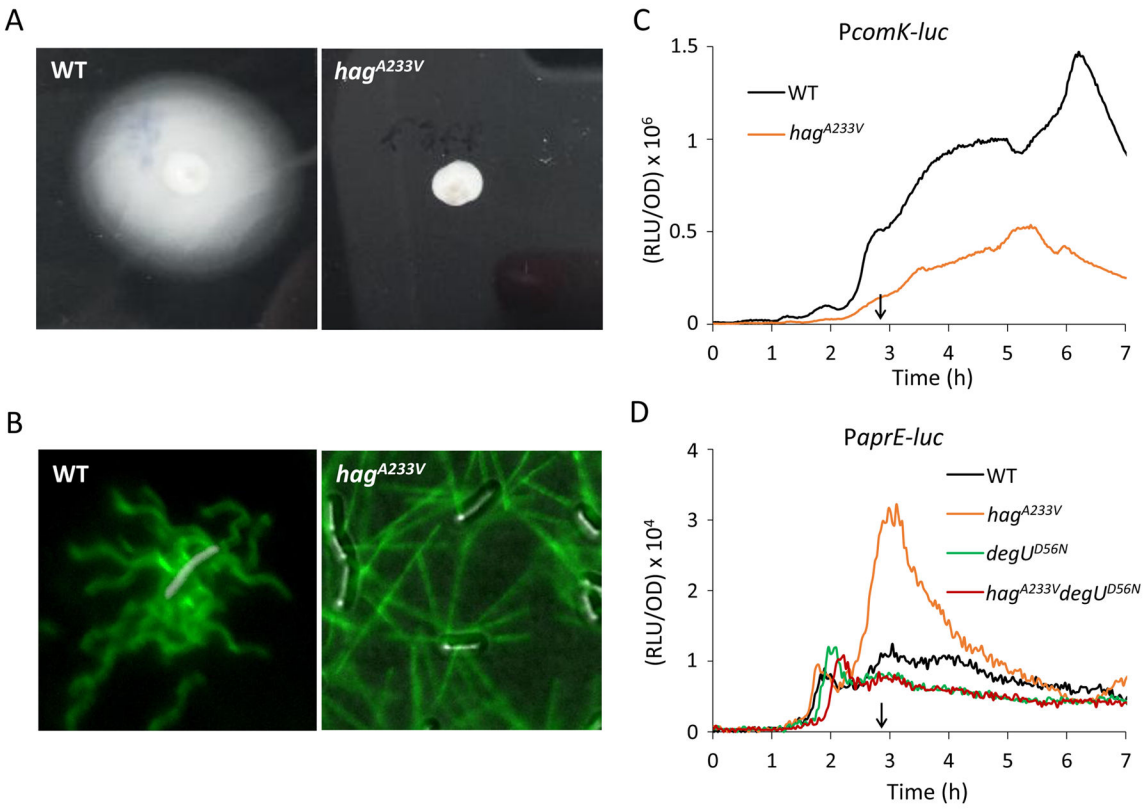

Figure 8.

Cells with straight filaments have increased DegU-P levels. (A) The nonmotile phenotype of a *hag*^{A233V} mutant. The wild-type (IS75) and the *hag*^{A233V} mutant (BD7599) were centrally inoculated on LB fortified with 0.3% agar. After 18 h incubation at 30°C, the plates were photographed against a black background. (B) Fluorescence microscopy of flagella filaments (Hag^{T209C}). Hag^{T209C} was stained with a maleimide reactive dye (green) in the wild-type strain (BD7816, *hag*^{T209C}) and the *hag*^{A233V} mutant (BD7757, *hag*$^{T209C\text{-}A233V}$). Strains were grown to mid log phase in LB. (C) *hag*^{A233V} decreases *comK* expression. Effect of *hag*^{A233V} (BD7626) on P*comK-luc* expression compared to wild-type (BD4773). (D) *degU*^{D56N} suppresses high *aprE* expression in *hag*^{A233V}. Expression from P*aprE-luc* in *hag*^{A233V} is higher than wild-type expression. The *degU*^{D56N} allele bypasses *hag*^{A233V} for expression from P*aprE*. Strains used were: wild-type P*aprE-luc* (BD6904), *hag*^{A233V} P*aprE-luc* (BD8007), *degU*^{D56N} P*aprE-luc* (BD7423), and *hag*^{A233V} *degU*^{D56N} P*aprE-luc* (BD8011). The vertical arrows in panel C and D indicate T_0.

Table 1

Transformation frequencies

strain	Relative transformation frequency[a]
IS75	$2.1x10^{-01} \pm 0.093$
Δ*hag* (BD7309)	$2.3x10^{-02} \pm 0.006$

[a]Transforming DNA was incubated with competent cells for 30 min before plating for leucine prototrophy. The mean and standard deviation of three experiments is shown.

Table 2

Motor measurements

	wild type (BD8207), n=11	***hag* (BD8263), n=17**	***hag*^{A233V} (BD7757), n=15**
Cell length (μm)	3.3 ± 0.2	4.6 ± 0.4	4.1 ± 0.2
Cell width (μm)	1.4 ± 0.1	0.9 ± 0.1	1.5 ± 0.1
Speed (Hz)	0.8 ± 0.2	0.7 ± 0.2	0.4 ± 0.1
Torque (pN-nm)	353 ± 117	341 ± 68	248 ± 38

The standard errors have been indicated.